Multipactor suppressing titanium nitride thin films analyzed through XPS and AES

M. Castro-Colin, W. Durrer, J.A. López, and L.A. Pinales
Physics Department, University of Texas,
El Paso, El Paso, TX 79968, USA.

C. Encinas Baca and D. Moller
Centro de Materiales Avanzados,
Chihuahua, Chihuahua, México

Recibido el 14 de mayo de 2007; aceptado el 26 de octubre de 2007

Cathodic-magnetron-deposited titanium nitride films were grown on anodized aluminum substrates and studied via AES and XPS spectroscopies to determine their depth-dependence composition. As it is well known, the native oxide grown on aluminum does not make the substrate impervious to radio frequency damage, and typically a thin film coating is needed to suppress substrate damage. In this article we present the profile composition of titanium nitride films, used as a protective coating for aluminum, that underwent prior conditioning through anodization, observed after successive sputtering stages.

Keywords: Thin film; magnetron deposition; multipactor; XPS; AES; anodization.

Películas de nitruro de titanio fueron depositadas utilizando un método magnetrón-catódico sobre sustratos de aluminio anodizado y estudiadas via AES así como XPS, para determinar la composición de las películas en función del grosor. Como es sabido, el óxido natural que crece sobre aluminio es susceptible al daño por radio frecuencias, de modo que es necesario suprimir tal daño por medio de un recubrimiento. En este artículo presentamos el perfil de composición de películas de nitruro de titanio, utilizadas como recubrimiento protector de aluminio, estudiadas trás la aplicación de etapas sucesivas de sputtering; las películas fueron previamente anodizadas.

Descriptores: Películas delgadas; deposición via magnetrón; multipactor; XPS; AES; anodización.

PACS: 79.20.Fv; 79.20.Rf; 79.60.-i; 81.15.-z; 82.45.Cc; 81.70.Jb

1. Introduction

The multipactor effect is a phenomenon that exists in devices where free electrons can resonate while interacting with an alternating electric field. The interaction can lead to exponential multiplication of electron emission which could ultimately deteriorate the device, thus the importance of impeding such phenomenon [1].

Multipactor starts with the impact of an electron on a surface which can release one or more secondary electrons into the vacuum. Such electrons can then be accelerated by radio-frequency (RF) fields [1–3] that will lead the angular and energy parameters of the impinging electron and impact the surface, starting the process again if conditions are favourable. Under some circumstances the number of electrons released will have a sustained multiplication of the number of electrons, leading to exponential growth of the electron yield [4, 5]. The multiple emission of electrons can not be sustained by the device and surface damage follows.

There are several methods to suppress or diminish the multipactor process [6–9], yet the best alternative for multipactor suppression seems to be the coating of the RF window with a preventive thin film of relatively effective materials.

One of the multipactor suppression methods, titanium nitride coating [10–12] by laser deposition, has been demonstrated to be effective at reducing secondary electron emission, presumably by shortening the mean free paths for electrons [13]. In this study the properties of thin film coatings of titanium nitride magnetron-deposited will be investigated to appreciate the structure of coatings that successfully suppress multipacting.

The composition of the thin films will be analyzed using X-ray photoelectron spectroscopy (XPS) and Auger electron spectroscopy (AES) [14, 15], after successive sputtering of the surface to better understand their composition gradient down to the substrate.

2. Fabrication of the thin films

The titanium nitride thin films were fabricated using magnetic assisted cathodic erosion [16] (also referred to in the text as cathodic-magnetron deposition) on anodized aluminum plates. The samples were produced at Centro de Investigación en Materiales Avanzados (CIMAV) [16] using a Intercovamex chamber, model V3, equipped with four sources.

The vacuum was infused with nitrogen gas of 1.0 to 6.5 cm^3/min and argon gas of 1.5 cm^3/min. The substrate to target distance was 7 cm and the magnetic fields generated ensured ample plume coverage of the aluminum window plates. Chamber pressures ranged from 10^{-6} to 10^{-9} Torr and the temperatures of the substrate holder ranged from 300 ^{o}C to 400 ^{o}C. The working pressure was 2.0×10^{-3} Torr from a base pressure of 2.0×10^{-6} Torr and titanium of purity 99.999% was used. Unlike what is done in similar experiments, no current was applied to the substrate during deposi-

TABLE I. Deposition conditions of titanium nitride thin film coatings. The subindex x in TiN_x is not indicative of stoichiometry but simply a label.

Sample Conditions	TiN_1	TiN_2	TiN_3	TiN_4	TiN_5	TiN_6	TiN_7	TiN_8	TiN_9	TiN_{10}	TiN_{11}
T substrate (^oC)	400	400	300	300	300	300	300	400	400	400	400
P (base, Torr$\times 10^{-5}$)	2.2	2.6	0.13	0.22	1.3	2.1	0.09	2.7	2.7	6.2	4.9
P (work, Torr$\times 10^{-2}$)	2.4	2.2	0.75	1.2	0.82	0.71	0.8	0.84	1.90	0.95	0.95
Ar (cm^3/min)	5	1.9	5	5	5	5	1.5	1.5	1.5	1.5	1.5
N (cm^3/min)	15	15	2	5	2.5	2	5	5	5	5	5
Power (W)	90	80	80	80	80	80	80	80	80	80	80
Current (A)	0.24	0.28	0.27	0.25	0.26	0.26	0.24	0.24	0.27	0.25	0.25
Voltage (V)	329	286	293	323	306	310	326	335	300	321	314
Film Depth (A)	40	32	36	14	39	41	189	136	84	78	135

tion and the plate was fixed. To obtain the best deposition conditions, firstly the most appropriate combination of growth parameters had to be determined [16]. Table I shows various typical deposition conditions.

Anodization was used to coat the surfaces to prepare them for the titanium nitride coating. The substrate was placed in an acid while a current was applied, and the acid would be stirred to prevent temperature layering. The oxide layer depth formed on the plates, in the μm range, can be estimated using the current density and exposure time [17]. The process changes the microscopic texture of the surface which is likewise imprinted onto the thin coating and exhibited through a change in the crystal structure; no mention is made of the crystallinity aspect of the thin films in the present article.

3. Methodology

AES and XPS are used to gain information on surface chemical composition, concentration, and surface bonding states. These techniques are well know in surface analysis and constitute a powerful analytical technique for modern surface science [13].

As surface analysis requires clean surfaces free from contamination of different types, which usually arise from handling, manufacture, and ambient exposure. The surfaces in this study were prepared and maintained atomically clean by means of argon ion bombardment, *i.e.* by sputtering [13].

The application of AES, XPS and sputtering are presented next.

3.1. Auger Electron Spectroscopy

The spectral distribution is obtained by bombarding the sample with an electron beam and the Auger electrons are captured by the energy analyzer so that a graphical representation of electron signal versus kinetic energy can be obtained. In this instrument, the energy sweep can be performed from 0 to 2000 eV, and the sample is bombarded with a beam voltage of 2.0 kV with the filament energized to a standard emission control setting of 0.6 mA, and an electron beam current of approximately 0.2 μA.

The energy analyzer, a cylindrical mirror analyzer (CMA) Perkin-Elmer Φ 25-270 AR energy analyzer, counts the number of Auger electrons collected at their respective energies and renders N(E) versus the energy of the electrons emitted off the surface. As it is customary, we present the differentiated spectra of the results obtained (through the software AugerScan, which uses the Savitzky-Golay algorithm) to yield dN(E)/dE. This provides a better way of detecting the small peaks superimposed on a large background. The change in gradient of the electron energy distribution can then be measured peak-to-peak and since the magnitude of the differentiated height is approximately proportional to the integrated area of the N(E) curve peak, this information can be used to find the relative surface elemental concentrations on the sample. The technique is sensitive enough to find monolayer and sub-monolayer species concentration [13].

Quantitative analysis is accomplished by comparison against known compositions. The sensitivity of the system is determined from the collection efficiency of the analyzer, incident beam current and energy, and the probability of Auger transitions.

To calculate the relative sensitivity, S_x, for element x, a comparison of a signal from a pure silver specimen and the one from the sample of interest are used. The relationship used that integrates these elements is:

$$S_x(E_p) = \left(\frac{A+B}{A}\right)\frac{I_x}{I_{Ag}K_x} \tag{1}$$

where A and B are the indices of the chemical formulation for X_A and Y_B, I_x and I_{Ag} are the magnitudes of the peak-to-peak amplitudes of the spectra, and K_x is the handbook scale factor of the element x, while $K_{Ag} = 1$. The relative elemental concentration of the sample surface is found through

$$C_x = \frac{\left(I_x S_x^{-1} d_x^{-1}\right)}{\sum_\alpha \left(I_\alpha S_\alpha^{-1} d_\alpha^{-1}\right)} \tag{2}$$

where the summation is made by counting the elemental

peaks over the entire spectrum, and d_x and d_α are the scale factors, that include instrumental settings. The experimental error arises from the difference in the system and the atomic work function, about 0.05%, which translates to about 1 eV. Sensitivity, scale factors, and Auger peaks can be found in reference [18].

3.2. X-Ray Photoelectron Spectroscopy

For this part of the analysis we use a Perkin-Elmer Φ 32-095 X-ray source control, where the magnesium anode with $h\nu = 1253.6$ eV is energized to 200 Watts at 15 kV, and the sample is then irradiated to obtain the spectral analysis. As with AES, the photoelectrons are collected and graphed, so that N(E), versus binding energy spectrum can be obtained.

XPS is complementary to AES as its spectra can show both Auger and photoelectron peaks. Sensitivity values are known to influence the concentration computation in XPS and for the equipment used they can be found in reference [19]. The concentration in XPS is given by

$$C_x = \frac{(I_x/S_x)}{\sum_\alpha (I_\alpha/S_\alpha)} \tag{3}$$

where the summation is made of one peak per element over the entire spectra, with all the peaks produced on the same scale.

3.3. Sputtering

Sputtering is done with the Perkin-Elmer PHI 560 ESCA/SAM system using argon gas of 99.98 % purity at 275 pounds per square inch (PSI), which was infused via a leak valve into an ionizing chamber at a standard ionizer emission current setting of 25 mA, in a nominal range of 1.5 to 15 mPa of pressure in the ionizing chamber, and propelled toward the film using a potential difference of up to 3.1 kV. The system can deliver a cascade of ions on region 500 μm × 500 μm or can be rastered over an area of up to a 1 cm × 1 cm. Argon ions, being massive particles, easily remove or strip away large particles, by comparison with less massive particles; therefore they were preferred in these kinds of experiments [20].

4. Results

The length of each sputtering session lasted from 30 minutes to one hour. The magnetron-erosion-deposited samples anodized with TiN at various time intervals, gave the relative atomic concentrations listed in Table II and illustrated in Figs. 2, 3, 4 and 5. The concentrations after several sputtering stages are those of Table III.

The magnetron-deposited titanium nitride films showed that when considering both spectra, AES and XPS, relative concentrations of carbon 1s, oxygen 1s, nitrogen 1s, and titanium $2p^3$ core Auger and photoelectron peaks, mutually corroborate the presence of these elements. The concentrations, shown in Table III, help to identify the Auger peaks on the AES spectra, which are obtained by averaging over ten measurements, followed by the calculation of the derivative (Figs. 2, 3, 4, and 5), and finally using the concentration formula given above. As it is well known, the derivative helps to better identify the Auger peaks from the background noise of inelastically scattered electrons expelled during the process. Figure 6 shows a typical, XPS, spectrum obtained from a 4-hour anodized sample. The concentrations using XPS, as is customary, are obtained by taking the peak total area above the height of the base, and then using the concentration formula for XPS shown above, to get the percentages relative to the total concentration of surface atoms detected.

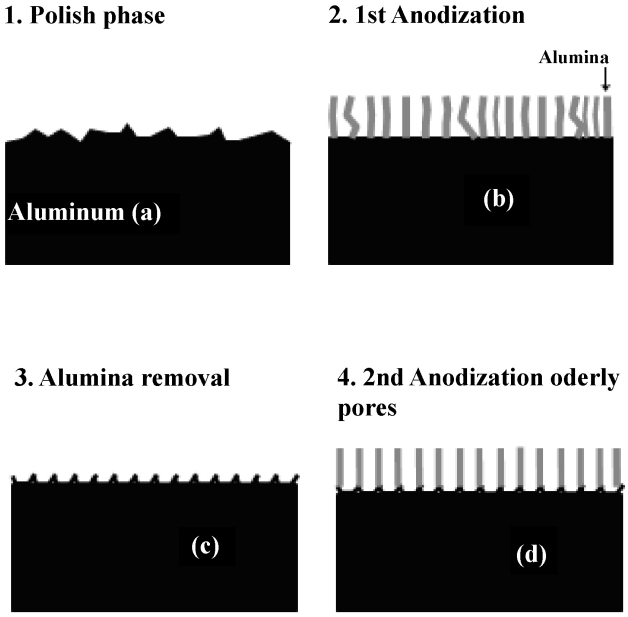

FIGURE 1. Schematic of the substrate manufacturing process. Thin films of titanium nitride are grown on substrates manufactured following four basic steps: polishing, first anodization, alumina removal, and second anodization. The samples analyzed were anodized for 4, 8, 12, and 24 hours.

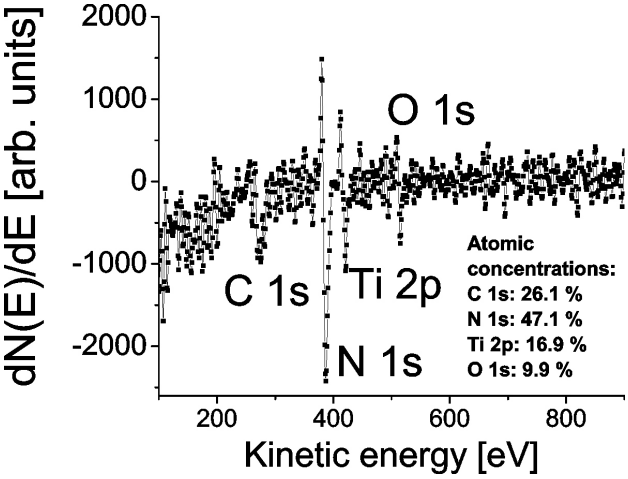

FIGURE 2. Derivative of AES survey after sputtering the sample anodized for 4 hours.

TABLE II. Initial conditions of anodized titanium nitride windows; four different times

Element	4 hr AES (%)	4 hr XPS (%)	8 hr AES (%)	8 hr XPS (%)	12 hr AES (%)	12 hr XPS (%)	24 hr AES (%)	24 hr XPS (%)
O 1s	14.1	29.7	14.3	15.9	15.9	15.9	11.6	15.9
Ti $2p^3$	15.5	17	15.4	9.1	15.4	9.1	14.9	9.1
N 1s	47.6	20	54	26.3	53.4	26.3	51.1	26.3
C 1s	22.7	33.3	15.3	48.8	15.3	48.8	22.4	48.8

TABLE III. Concentrations of anodized titanium nitride windows after final sputtering.

Element	4 hr AES (%)	4 hr XPS (%)	8 hr AES (%)	8 hr XPS (%)	12 hr AES (%)	12 hr XPS (%)	24 hr AES (%)	24 hr XPS (%)
O 1s	11.7	27.7	13.5	15.9	15.6	15.9	11.7	15.9
Ti $2p^3$	18.4	18.7	18.2	9.1	17.9	9.1	23.6	79.1
N 1s	52.6	21.2	52.2	26.3	48.9	26.3	40.2	26.3
C 1s	17.4	32.4	16.1	48.8	17.6	48.8	24.5	48.8

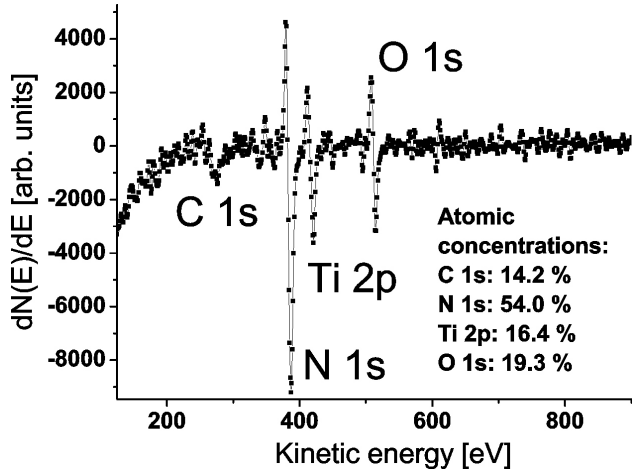

FIGURE 3. Derivative of AES survey after sputtering the sample anodized for 8 hours.

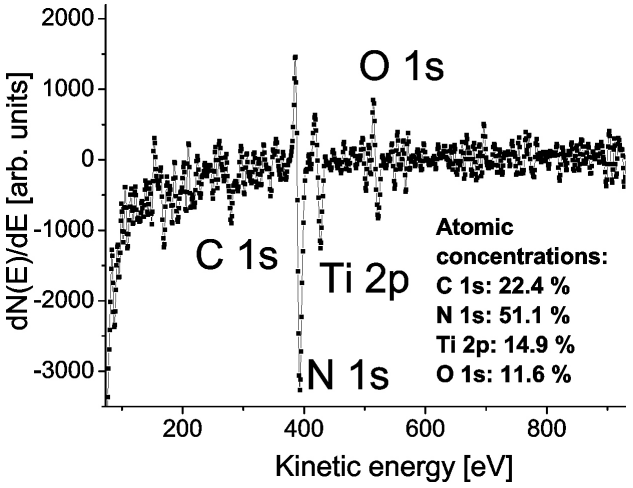

FIGURE 5. Derivative of AES survey after sputtering the sample anodized for 24 hours.

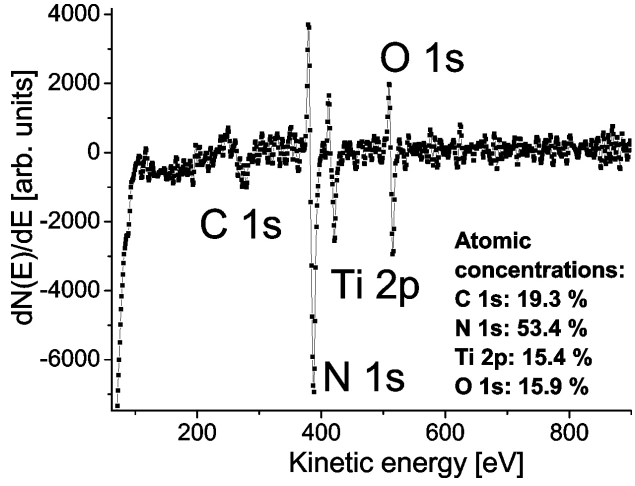

FIGURE 4. Derivative of AES survey after sputtering the sample anodized for 12 hours.

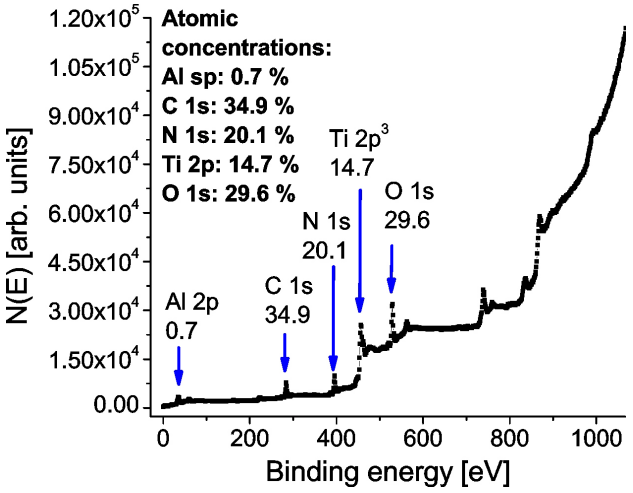

FIGURE 6. XPS survey of 4-hour anodized sample.

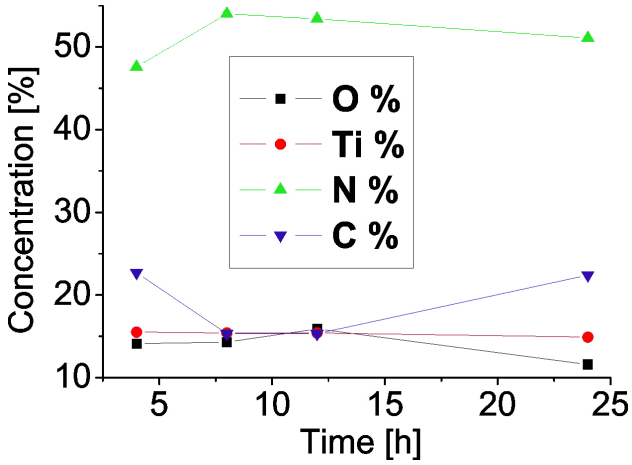

FIGURE 7. AES percentual composition of samples anodize for four times, before and after sputtering.

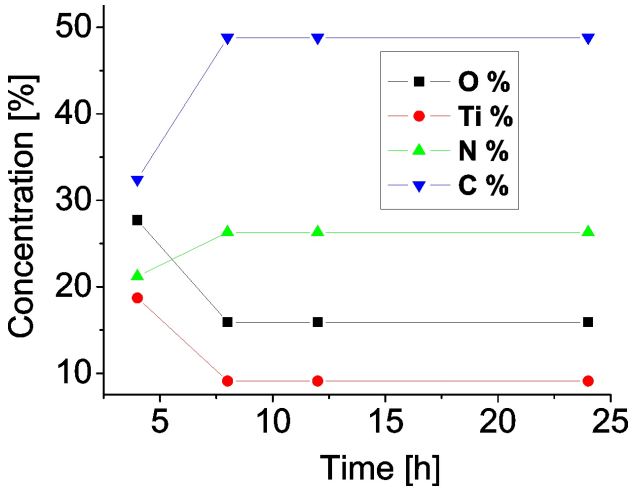

FIGURE 8. XPS percentual composition of samples anodize for 4, 8, 12, and 24 hours, after sputtering.

The tables of concentration, Tables II and III, give the initial and final concentrations of the respective windows using both the AES and XPS methods.

The 8-hour and 12-hour samples were not sputtered intensely like the 4-hour and the 24-four hour samples because the purpose was to examine the depth of the film. Therefore the least sputtered were sputtered intensely for periods of an hour each at standard Ar ion source settings of 1.5 mPa to 2.0 mPa, 3.0 kV, and 25 mA, directly in a 500 μm by 500 μm hole on the sample. The approximate depth analyzed was about 40.0 nm.

Figures 7, and 8, show the composition down to the surface-most 40 to 50 nm, from AES and XPS surveys, before and after sputtering. We can observe that there is larger variation in the 4-hour anodized samples

5. Summary and conclusions

A comprehensive study was done on the composition of anti-multipactor thin film coatings manufactured through magnetron erosion deposition on anodized aluminum substrates. The composition was shown to be homogeneous throughout the films, in this case with compositional variations within about 5 %, both in the wide and point area surveys. 8-, 12-, and 24-hour anodization samples showed a very similar composition, which varies from that of 4-hour anodized samples. This may be due to the roughness of the substrate, [16], induced by the anodization process.

The results show, Figs. 7 and 8, a relative concentration percentage decrease in oxygen 1s and carbon 1s and a constant in titanium $2p^3$ and nitrogen 1s from the original depth to the sputtered depth. The presence of oxygen 1s and carbon 1s may be due to the contamination of the samples after extraction, handling, transportation, and/or even during manufacturing and analysis. Oxygen from the anodization process, that is, from alumina layer, may desorb because of the plume interaction and bond later to the thin film.

Thicker films of titanium nitride showed greater homogeneity even after sputtering to an approximate depth of 50.0 nm. The graph of the XPS spectra over the sputtering regimes indicated a region of relative homogeneity and about 20 % variation from the initial. The variation is due to the mount's secondary electron emission and the vacuum residual influence, since XPS takes the spectra over the area directly under the beam.

The titanium nitride thin film showed a 1:1 relative even composition of titanium to nitrogen on all the windows for the initial and final stage of sputtering. All the films also show comparable concentrations of the elements identified, further supporting the idea that oxygen is desorbed and adsorbs back into the film throughout the process.

In general the film produced via this method show consistent homogeneity, judging by the compositional variation registered after successive sputtering, which makes them appropriate as anti-multipacting coatings.

1. J. Rodney and M. Vaughan. *Multipactor*, *IEEE Trans. Elec. Dev.* **35** (1988) 1172.

2. M. Golio, *Microwave and RF Product Applications*, (CRC Pressp LLC 2003) 1.

3. J.G. Power *et al.*, *Phys. Rev. Lett.* **92** (2004) 164801-1.

4. A. Modinos, *Field, Thermionic, and Secondary Electron Emission Spectroscopy* (Plenum Press 1984) 327.

5. R.A. Kishek, Y.Y. Lau, A. Valfells, and R.M. Gilgenbach, *Physics of Plasmas* **5** (1998) 2120.

6. F. Paschke, *J. Appl. Phys.* **32** (1961) 747.

7. V. Semenov, A. Kryazhev, D. Anderson, and M. Lisak, *Physics of Plasmas* **8** (2001) 5034.

8. R. Udiljak, D. Anderson, M. Lisak, V.E. Semenov, and J. Puech, *Physics of Plasmas* **11** (2004) 5022.

9. S. Riyopoulos, D. Chernin, and D. Dialetis, *Physics of Plasmas* **2** (1995) 3194.

10. K.M. Welch, *SLAC-174* (1974) 11.

11. W. Pamler, E. Wildenauer, A. Mitwalsky, *Surf. Interf. Anal.* **15** (1990) 621.

12. T. Sonoda, A. Watazu, K. Katou, and T. Asahina, *Microscopy and Microanalysis* **12** (2006) 356.

13. G. Attard and C. Barnes, *Surfaces* (Oxford University Press 1998) 1, 37.

14. J. Haupt, M.A. Baker, M.F. Stroosnijder, and W. Gissler, *Surf. Interf. Anal.* **22** (1994) 167.

15. Q.Y. Zhang, *J. Vac. Sci. Technol. A* **13** (1995) 2384.

16. C. Encinas Baca, *Crecimiento de películas delgadas de TiN en sustratos de alumina nano-porosa obtenidos mediante anonizado*, M.S. Tesis, CIMAV, Chihuahua, México, 2007.

17. V.F. Henley, *Anodic Oxidation of Aluminum & Its Alloys*, 1st Ed. (Pergamon Press, 1982) 1.

18. L.E. Davis, N.C. Macdonald, P.W. Palmberg, G.E. Riach, and R.E. Weber, *Handbook of Auger Electron Spectroscopy* 2nd Ed. (Perkin-Elmer Corporation, 1979) 1.

19. C.D. Wagner, W.M. Riggs, L.E. Davis, J.F. Moulder, and G.E. Muilenberg, *Handbook of X-Ray Photoelectron Spectroscopy* 2nd Ed. (Perkin-Elmer Corporation, 1979) 1.

20. D.P. Woodruff and T.A. Delchar, *Modern Techniques of Surface Science* 2nd Ed. (Cambridge University Press, 1994) 4, 105, 321.